Nature Environment and Pollution Technology
An International Quarterly Scientific Journal

p-ISSN: 0972-6268
(Print copies up to 2016)
e-ISSN: 2395-3454

Vol. 21 | No. 4 | pp. 1649-1656 | 2022

Original Research Paper

https://doi.org/10.46488/NEPT.2022.v21i04.017

Open Access Journal

Investigation of Adsorption of Heavy Metal Ions on C_3N_4 Nanosheets by Batch and Microscopic Methods

C. K. Fu*, Y. Fang*, C. Y. Yang*, C. G. Chen* and L. X. Wang*†

*Department of Chemistry and Chemical Engineering, Shaoxing University, Zhejiang 312000, P. R. China

†Corresponding authors: Linxia Wang; wlxsyx@163.com

Nat. Env. & Poll. Tech.
Website: www.neptjournal.com

Received: 17-11-2021
Revised: 16-02-2022
Accepted: 24-02-2022

Key Words:
Heavy metals
C_3N_4
Adsorption
Nd(III)
Th(IV)

ABSTRACT

This paper mainly studies the adsorption of C_3N_4 on a series of heavy metals and focuses on the adsorption performance of C_3N_4 on Nd and Th. The main conclusions are as follows: Through the use of the thermal stripping method and melamine as the raw material, C_3N_4 was obtained at a lower cost, with superior adsorption performance. Through SEM-EDS, TEM, and other characterization analyses, the results show that C_3N_4 has a clear multilayer sheet structure, and the surface of the material is more uniformly dispersed. The maximum adsorption capacity of C_3N_4 for Th is 86.6 $mg.g^{-1}$, and the maximum adsorption capacity for Nd is 60.1 $mg.g^{-1}$. The kinetic model is also used for fitting, and the results showed that the kinetic of the adsorption was in line with the pseudo-second-order model, indicating that the adsorption was chemical interaction. After C_3N_4 adsorbed heavy metal elements, it was characterized by SEM-EDS, TEM, UHRTEM, and AFM. The results showed that a variety of heavy metal ions can be adsorbed by C_3N_4, which proved that C_3N_4 has good adsorption performance. Due to factors such as metal particle size, the adsorption of C_3N_4 on heavy metal elements is different.

INTRODUCTION

With the rapid development of economic globalization, the use of heavy metals by humans is increasing, which has led to an increasingly serious problem of heavy metal pollution. At present, the problem of heavy metal ions pollution is widespread in all regions of our country (Li et al. 2015), which has already caused a serious impact on the environment. In addition, heavy metal ions have the characteristics of concealment, long-term, and irreversibility (Li et al. 2014). There will be serious enrichment in the human body (Xu et al. 2016), so it can still cause huge health risks at low concentrations. Moreover, different heavy metal ions have different hazards to the human body. Excessive lead (Pb) content can easily lead to neurological disorders, induced anemia, and other diseases (Islam et al. 2014). Neodymium (Nd) and thorium (Th) two rare earth elements are low for a long time Dose exposure and intake will have adverse consequences for human health or metabolism in the body, and even cause lung and liver diseases (Ahmad et al. 2019, Talip et al. 2009). Moreover, the unreasonable exploitation of neodymium (Nd) and thorium (Th) will also lead to the destruction of the ecological environment, and cause problems such as the greenhouse effect and the acidification effect.

Therefore, finding a convenient, economical, and effective method to deal with heavy metal pollution has become one of the key areas of research by scientists in the world. To date, various technologies have been proposed and practiced, such as ion exchange, membrane filtration, chemical precipitation, adsorption, etc. Considering the removal efficiency of heavy metal ions and the convenience of operation, the adsorption method is favored by many researchers (Zheng et al. 2007). Its main mechanism is that when the fluid passes through the adsorbent, the molecules and ions in the fluid will accumulate on the adsorbent. Moreover, the adsorption method has the characteristics of green and environmental protection, which is simpler and more efficient than other methods. In recent years, new adsorbents have been continuously developed and applied, and the choice of adsorbents has increased year by year. Carbon nanomaterials are the most common type among them. Common carbon nanomaterials include activated carbon (Bali & Tlili 2019), fullerene (Alekseeva et al. 2016), and carbon nanomaterials. Nanotubes (Tian et al. 2012), graphene materials (Zhao et al. 2011), etc. The above-mentioned adsorbents have been widely reported as effective adsorbents (Liao et al. 2018), and because of its special properties, C_3N_4 is widely used in photocatalysis, electrocatalysis, bioimaging, heavy metal adsorption, and other fields, and it is often used as a precursor to synthetic

composite materials. For example, Zheng et al. (2011) used a composite of C_3N_4 and porous graphite to prepare high-efficiency electrocatalysts, which have better methanol tolerance and higher catalytic efficiency than current commercial products. Hu et al. (2020) also found that g- C_3N_4 nanosheets have higher catalytic efficiency in the field of photoelectric catalysis. Compared with ordinary graphene materials, the ultra-thin g- C_3N_4 nanosheets prepared by Zhang et al. (2013) enhanced the light responsiveness of the material in aqueous solutions, which makes g- C_3N_4 also have greater application prospects in the field of bioimaging. Furthermore, Wang et al. (2017) found that g- C_3N_4 under the synergistic effect of photocatalysis and adsorption can remove Cr(VI) more efficiently, with a degradation rate of 100% at low concentrations. Similarly, Shen et al. (2015) found that g- C_3N_4 has a good adsorption effect on heavy metal elements such as Pb(II), Cu(II), Cd(II), Ni(II), and the adsorption kinetics all follow the pseudo-secondary model.

Based on the above facts and analysis, this thesis will study the following three aspects: First, use the thermal stripping method to prepare melamine into C_3N_4, and perform SEM-EDS and TEM characterization analysis on the prepared C_3N_4; secondly, use the prepared C_3N_4 Adsorbent, to study the adsorption effect and mechanism between C_3N_4 and heavy metal ions, and determine its adsorption performance, optimize the experimental conditions; finally, the C_3N_4 after adsorbing different heavy metal elements is characterized by SEM-EDS, TEM, UHRTEM and AFM, and other methods Process and analyze the adsorption of C_3N_4 on different types of metals.

MATERIALS AND METHODS

Experimental Materials and Apparatus

Hydroxylamine hydrochloride, sulfamic acid, citric acid, disodium hydrogen phosphate, arsenazo III, and melamine were provided by Shanghai Aladdin Biochemical Science and Education Co., Ltd. Neodymium nitrate hexahydrate, thorium oxide, sodium hydroxide, and hydrochloric acid were provided by Shanghai Ling Feng Chemical Reagent Co., Ltd. The purity of the reagents is analytically pure, and the deionized water is self-made. The components of the buffer solution obtained are citric acid and disodium hydrogen phosphate, and the components of the reducing agent are hydroxylamine hydrochloride and sulfamic acid.

Electronic balance (AL204) and pH meter (Five Easy plus) are produced by Mettler-Toledo (Shanghai) Co., Ltd. The ultrasonic cleaner (KQ5200DA) is produced by Kunshan Ultrasonic Instrument Co., Ltd. UV-Vis spectrophotometer (SP-756P) is produced by Shanghai Spectrometer Co., Ltd. And the vacuum drying oven (DZF-6020) is produced by Shanghai Jinghong Experimental Equipment Co., Ltd. The desktop low-temperature constant-temperature shaking shaker adopts the German IKA KS4000i control shaker. Use the muffle furnace (KSL-1700) produced by Hefei Kejing Material Technology Co., Ltd., And the micro-continuous adjustable pipette (7010101017) produced by Dalong Xingchuang Experimental Instrument (Beijing) Co., Ltd., experimental method

Preparation of C_3N_4 Adsorbent

Prepare a dry and impurity-free alumina crucible, weigh 20g of melamine raw material into it with an electronic balance, spread the powder evenly in the crucible, and raise it to 520°C at a heating rate of 3°C.min^{-1} in a muffle furnace. After baking for 3 hours, the temperature is reduced from 520°C to room temperature at a cooling rate of 3°C.min^{-1} to complete the first thermal stripping treatment. Then put it into the muffle furnace, and repeat the above-mentioned roasting process, after the treatment is completed, take out the block-like light yellow powder C_3N_4. Transfer C_3N_4 to an agate mortar and grind into a fine powder, bag it for later use.

Static Adsorption Experiment

Take several 150 mL reaction flasks, use a pipette to accurately pipette the quantitative heavy metal ion standard solution into the reaction flask, add deionized water to make the total volume of the solution 100 mL, and adjust with 0.1 mol.L^{-1} HCl and 0.1 mol.L^{-1} NaOH respectively the pH of the solution is such that it has a pH gradient. After adding quantitative C_3N_4, use an ultrasonic cleaning machine for 30min ultrasonic treatment, and place it in a desktop low-temperature constant temperature shaking shaker for 24h after ultrasonication. Detect the influence of different pH on the adsorption of heavy metal ions. Choose several 150 mL reaction flasks. Accurately pipette the quantitative heavy metal ion standard solution into the reaction flask, add deionized water to make the solution volume 100 mL, and adjust the pH with 0.1 mol.L^{-1} HCl and 0.1 mol.L^{-1} NaOH respectively to make the pH value the same. Finally, C_3N_4 adsorbents of different qualities were added respectively, and ultrasonic treatment was carried out with an ultrasonic cleaning machine for 30 min. After ultrasonication, they were placed in a desktop low-temperature constant-temperature shaking shaker for 24 h to detect the influence of different adsorbent qualities on the adsorption of heavy metal ions. Select several 150 mL reaction flasks, respectively pipette different heavy metal ion standard solutions into the reaction flasks, add deionized water to make the reaction system 100 mL, and adjust the pH with 0.1 mol.L^{-1} HCl and 0.1 mol.L^{-1}

NaOH, Make the pH the same. Add quantitative C_3N_4, use an ultrasonic cleaning machine for 30min ultrasonic treatment, and place it in a desktop low-temperature constant-temperature shaking shaker for 24 h after ultrasonication. After the oscillation is complete, take 1 mL of the above solution in a 25 mL colorimetric tube. The volume is adjusted to 25 mL, and the absorbance is measured with an SP-756P UV-visible spectrophotometer.

Adsorption Experiment Data Processing

Calculate the adsorption capacity (q_e) of different sets of data. The adsorption capacity refers to the concentration of heavy metal ions adsorbed per gram of adsorbent. Adsorption capacity: $q_e=m_e/M$ where m_e(mg) represents the mass of heavy metal ions adsorbed, and M (mg) represents the mass of adsorbent.

In kinetic equation research, the three kinetic fitting models used in this experiment are fitted (pseudo-first-level model fitting, pseudo-second-level model fitting, and Elovich model fitting). The kinetic model is fitted to the experimental data according to the following formula (Chen et al. 2021, Wu et al. 2021):

Pseudo first-level model fitting: $In(q_e-q_t)=Inq_e-k_1t$

Pseudo secondary model fitting: $t / q_t = 1 / (k_2qe^2) + t / q_e$

Elovich model fitting: $q_t=1/\beta\cdot ln\alpha\beta+1/\beta\cdot ln^t$

Where q_e refers to the adsorption capacity ($mg.g^{-1}$) of the adsorbent after reaching the adsorption equilibrium, and q_t refers to the adsorption capacity of the adsorbate on the adsorbent at time t ($mg.g^{-1}$);

The pseudo first-order kinetic adsorption rate constant is k_1 ($1.min^{-1}$), k_2 ($g.m^{-1}.min^{-1}$) is the pseudo-second-order kinetic adsorption rate constant, α ($g.m^{-1}.min^{-1}$) and β ($g.mg^{-1}$) represent respectively Initial adsorption rate constant and desorption rate constant.

Characterization Method

In this study, JEOL, JSM-6360LV Scanning electron microscope-energy spectrum (SEM-EDS) was used for SEM characterization to analyze the morphological characteristics of the solid surface. The transmission electron microscope (TEM) can observe the finer structure of the sample, as well as the microstructure inside the material. After the team dispersed the samples evenly, they used the JEM-101 transmission electron microscope of JEOL for TEM characterization. The high-resolution transmission electron microscope (UHRTEM) can analyze the morphology, interface, and crystal defects of the material, and combine the morphology information with the structure information to analyze the material's particle size, growth orientation, and other properties. The instrument model used to test UHRTEM: JEM-2100F high-resolution transmission electron microscope produced by JEOL. To analyze the surface roughness measurement, surface size, and statistical processing of pits and protrusions, this study used the Atomic force microscope (AFM) of the Brooker dimension icon for characterization.

RESULTS AND DISCUSSION

In this study, the kinetic experimental conditions for Th(IV) were pH=3.0, adsorbent 40 mg, 200 mL 80 ppm Th solution, and Nd(III) kinetic experiment conditions were pH=5.5, adsorbent 80 mg, 200 mL 80 ppm Nd solution. Kinetic discussion, Fig. 1A shows the adsorption time curve of C_3N_4 on Th(IV) and Nd(III). It can be seen from the figure that the adsorption effect of C_3N_4 on Th(IV) and Nd(III) is obvious. As time increases, the amount of adsorption gradually increases. The adsorption rate is faster from 0 to 50 minutes, and the adsorption amount does not change much after 50 minutes, which tends to reach the adsorption equilibrium. The maximum adsorption capacity of C_3N_4 for Th(IV) is $86mg.g^{-1}$, the maximum adsorption capacity for Nd(III) is $60 mg.g^{-1}$, and the adsorption equilibrium time is 50min. Fig. 1B shows the fitting of the pseudo-first-order model of C_3N_4 adsorption of Th(IV) and Nd(III); Fig. 1C shows the fitting of the pseudo-second-order model of C_3N_4 adsorption of Th(IV) and Nd(III); Fig. 1D shows the Elovich model fitting of C_3N_4 adsorption of Th(IV) and Nd(III). It can be seen from the figure that the adsorption of Th(IV) and Nd(III) by C_3N_4 is in line with the pseudo-second-order model fitting, indicating that the adsorption experiment is chemical adsorption.

Scanning Electron Microscope Band Energy Spectrum (SEM-EDS) Analysis

Fig. 2 and Fig. 3A, B, C, and D respectively represent C_3N_4 and its SEM-EDS images after adsorption of Nd, Th, Cd, and Co. It can be seen from the figure that the C_3N_4 before the adsorption of heavy metal ions has an obvious multilayer flake structure and a large number of defects, and the dispersion is relatively uniform. After the heavy metal ions are adsorbed, it can be seen that part of the defects on the C_3N_4 surface is filled, and from the EDS spectrum, it can be seen that the four heavy metal elements are enriched in the defects on the C_3N_4 surface. It can be inferred that the heavy metal ions are successfully adsorbed on the C_3N_4 surface.

Transmission Electron Microscopy (TEM) Analysis

Fig. 4A, B, C, and D are TEM images of C_3N_4 under the transmission electron microscope and its adsorption of Cu, Pb, and Zn. It can be seen from the figure that there are a large

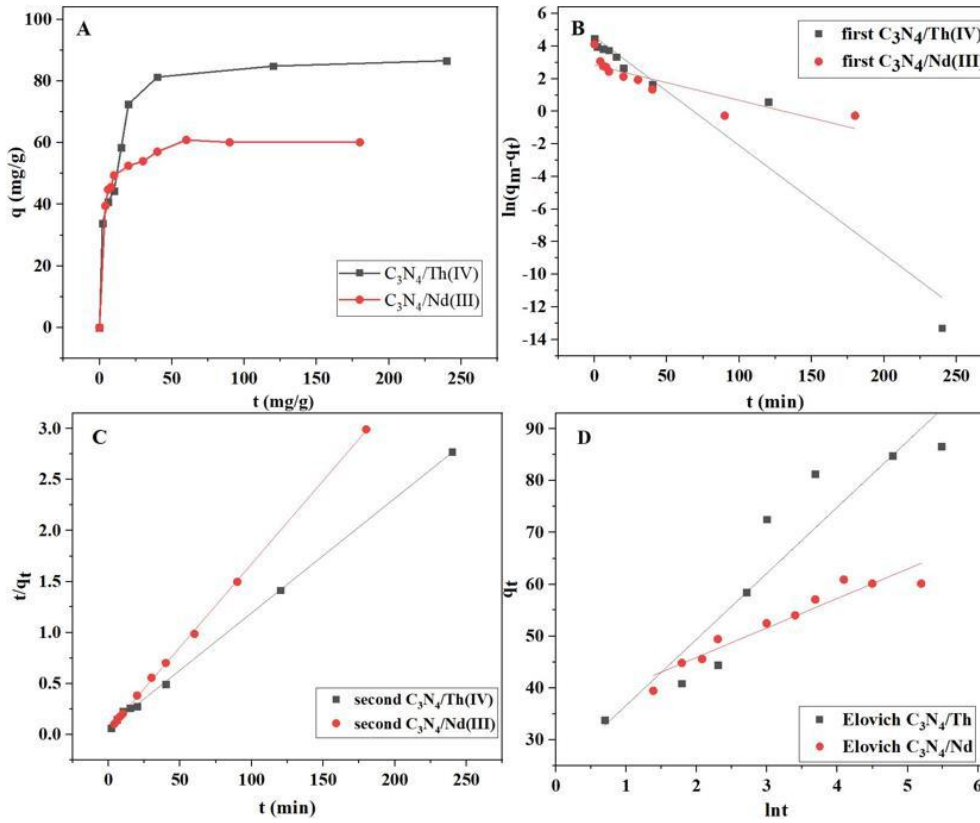

Fig. 1: C_3N_4 adsorption time curve for Th(IV) and Nd(III) (A), pseudo-first-order model fitting (B), pseudo-second-order model fitting (C), Elovich model fitting (D).

number of defects in the adsorbent. After the heavy metal ions are adsorbed, a large amount of material accumulation can be seen on the surface defects of C_3N_4, and it can be inferred that the heavy metal elements have been adsorbed.

High-Resolution Transmission Electron Microscope (UHRTEM) Analysis

Fig. 5 is the UHRTEM image of Cu(II) adsorbed by C_3N_4. According to the image obtained by high-resolution transmission electron microscope and energy spectrum analysis, it can be clearly observed from the characterization image that Cu(II) fills part of the defects, and it can be seen from the energy spectrum, Cu(II) is enriched in the defects of C_3N_4 surface. so it can be inferred that Cu(II) is successfully adsorbed on the C_3N_4 surface.

Atomic Force Microscopy (AFM) Analysis

Fig. 6 A, B, C, and D are the AFM images of C_3N_4 after adsorbing Nd, Th, Cd, and Co, respectively. It can be seen from the 3D diagram in Fig. 4-6 that C_3N_4 has an obvious three-dimensional structure. In addition, in the 2D image, the color depth can represent the height of the area, the darker area has a larger height, and the darker area has a smaller height. According to the above method, the three-dimensional structure of C_3N_4 can also be observed. As shown in Fig. 4-6 A2 and C2, the height of C_3N_4 is about 3.3nm, while Fig. 4-6 B2 and D2 show that the height of C_3N_4 is about 1.6nm. This may be due to the partial overlap of C_3N_4 in the A2 and C2 pictures, resulting in a large difference in local thickness.

CONCLUSION

Based on the above analysis, this paper describes the preparation and characterization process of C_3N_4, and explores the adsorption performance of C_3N_4 on heavy metals such as Nd, Th, Co, Cu, and focuses on the optimal pH, the amount of adsorbent, and reaction kinetics experiment was carried out. Finally, the adsorption effect of C_3N_4 on a variety of heavy metals was analyzed through the characterization image. conclusion as below:

(1) The adsorbent C_3N_4 was prepared by thermally peeling melamine, and it was characterized by SEM-EDS, TEM, and other methods. The results showed that the material

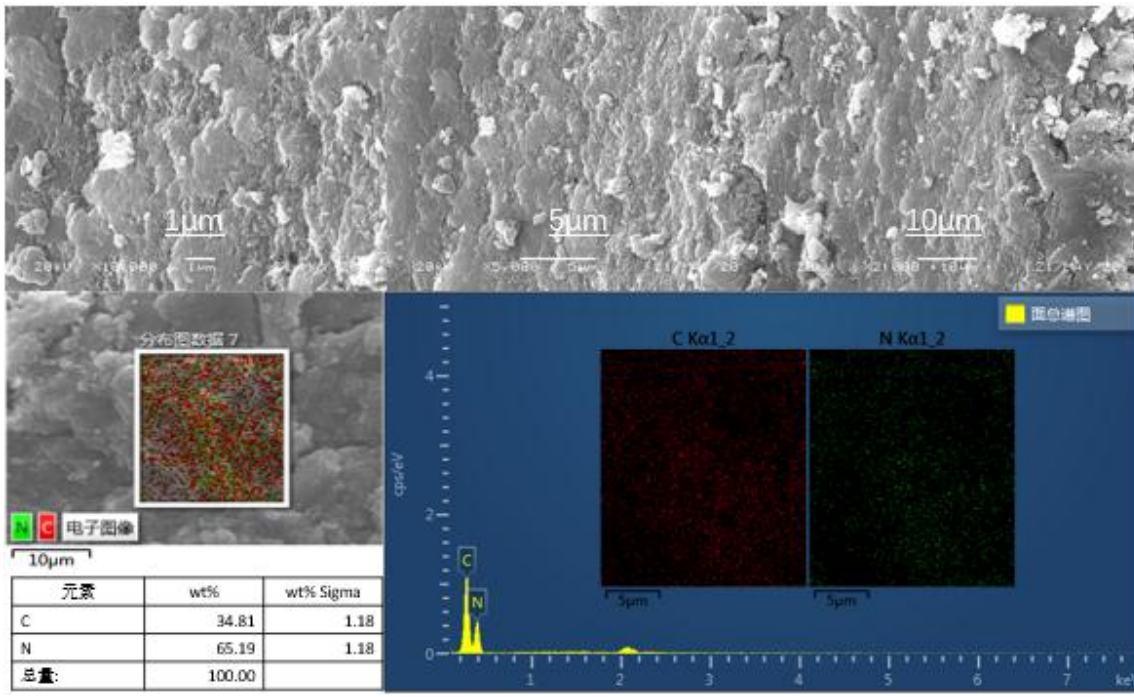

元素	wt%	wt% Sigma
C	34.81	1.18
N	65.19	1.18
总量:	100.00	

Fig. 2: SEM-EDS image of C_3N_4.

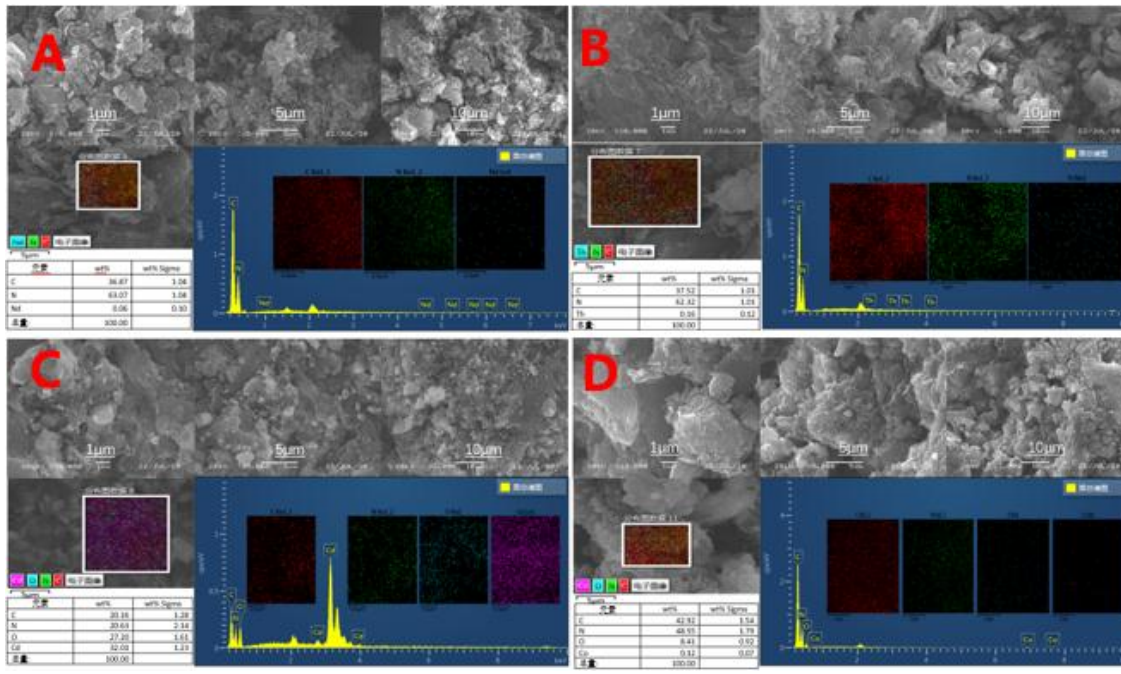

Fig. 3: SEM-EDS image of Nd adsorbed by C_3N_4 (A), SEM-EDS image of Th adsorbed by C_3N_4 (B), SEM-EDS image of Cd adsorbed by C_3N_4 (C), SEM-EDS image of Co adsorbed by C_3N_4 (D).

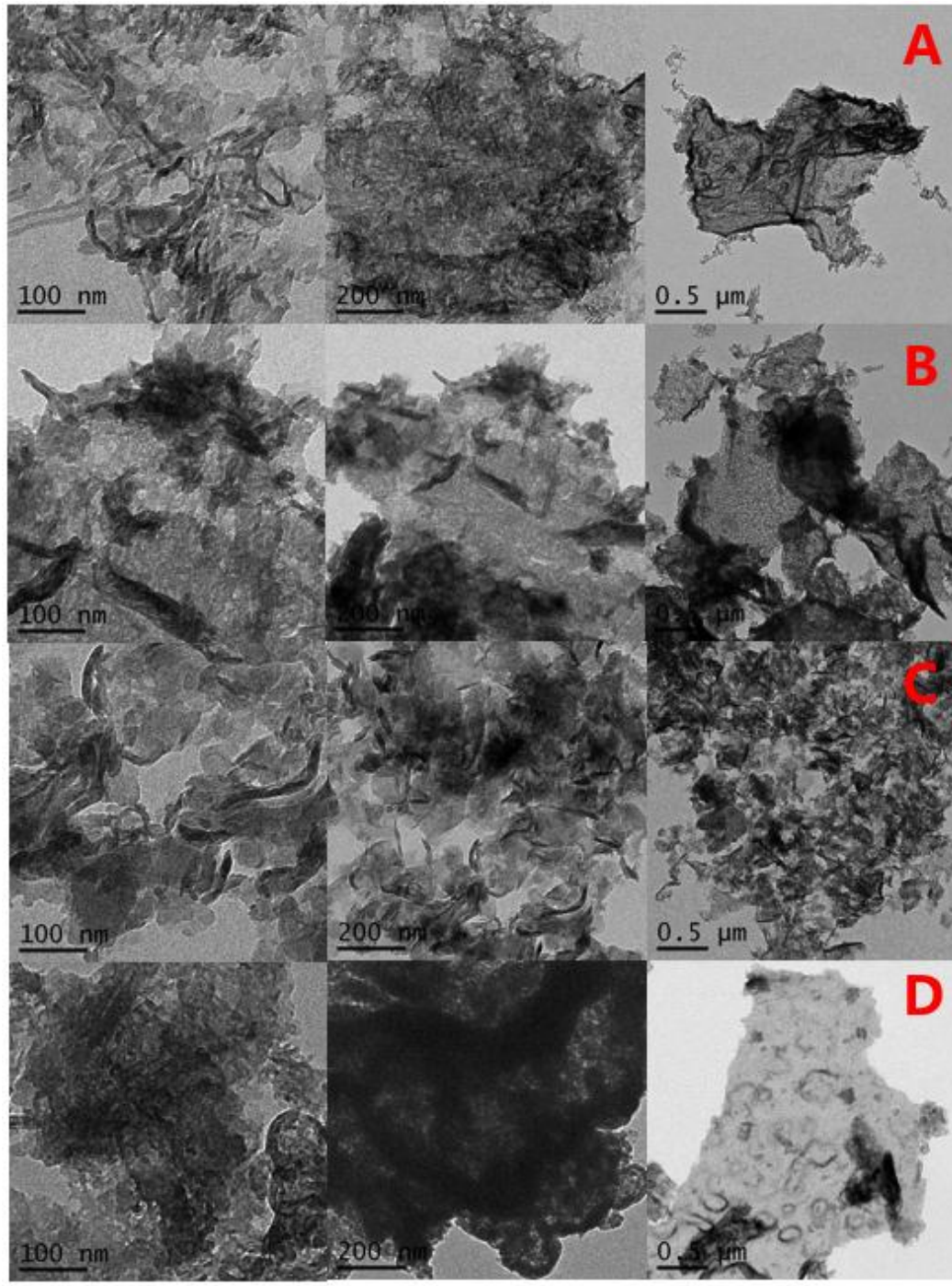

Fig. 4: TEM image of C_3N_4 (A), TEM image of C_3N_4 after adsorption of Cu (B), Pb (C), and Zn (D), respectively.

has a clear lamellar structure, the dispersion is relatively uniform, and the state of layered accumulation is not obvious.

(2) Using C_3N_4 as the adsorbent, it adsorbed heavy metal elements such as Nd, Th, Co, Cu, etc. And through SEM, TEM, UHRTEM, AFM, and other characterization methods. It is proven that C_3N_4 has relatively good adsorption performance for heavy metal elements.

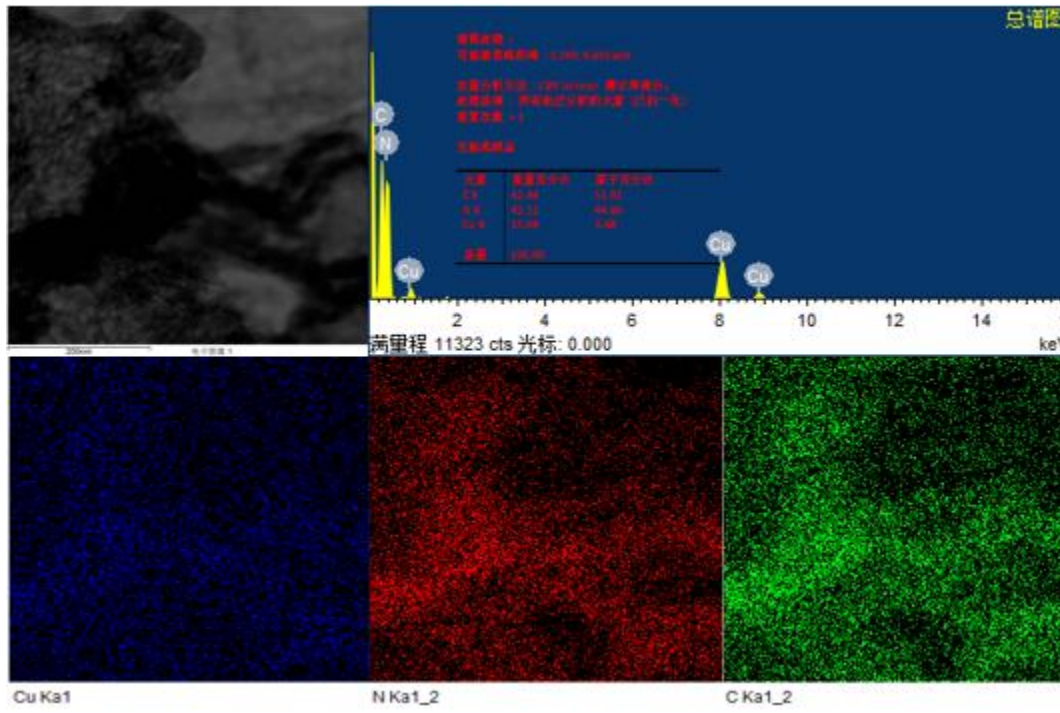

Fig. 5: UHRTEM image of Cu adsorbed by C_3N_4.

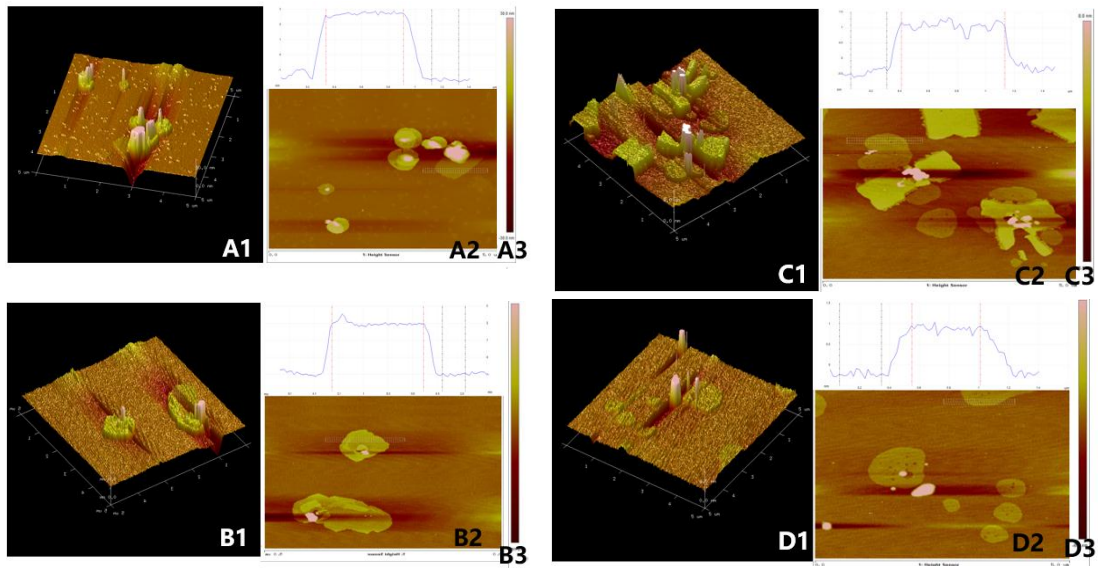

Fig. 6: AFM image after C_3N_4 adsorbed Nd (A), AFM image after C_3N_4 adsorbed Th (B), AFM image after C_3N_4 adsorbed Cd (C), AFM image after C_3N_4 adsorbed Co (D).

(3) Based on the C_3N_4 adsorbent, the influencing factors such as pH, adsorbent dosage, and heavy metal ion concentration for the adsorption of Nd and Th are explored. Finally, combined with pH=5.5, adsorbent mass of 80 mg, and Nd solution concentration of 80 ppm, the adsorption experimental kinetics of the Nd element is explored. Similarly, under the conditions of pH=3, adsorbent mass equal to 40mg, and Th solution concentration of 40 ppm, Exploring the dynamics of Th element. The investigation results show that the kinetic

fitting of the adsorption experiment is in accordance with the pseudo-second-order model fitting, indicating that the adsorption experiment is chemical adsorption.

REFERENCES

Ahmad, Z.U., Yao, L., Wang, J., Gang, DD., Islam, F., Lian, Q. and Zappi, M.E. 2019. Neodymium embedded ordered mesoporous carbon (OMC) for enhanced adsorption of sunset yellow: Characterizations, adsorption study, and adsorption mechanism. Chem. Eng. J., 359: 814-826.

Alekseeva, O.V., Bagrovskaya, N.A. and Noskov, A.V. 2016. Sorption of heavy metal ions by fullerene and polystyrene/fullerene film compositions. Prot. Met. Phys. Chem. Surf., 52(3): 443-447.

Bali, M and Tlili, H. 2019. Removal of heavy metals from wastewater using infiltration-percolation process and adsorption on activated carbon. Int. J. Environ. Sci. Technol. (IJEST), 16(1): 249-258.

Chen, J., Wu, H., Xu, L., Li, M., Du, K. and Sheng G. 2021. New insights into colloidal GO, Cr (VI), and Fe (II) interaction by a combined batch, spectroscopic, and DFT calculation investigation. J. Mol. Liq., 337: 116365.

Hu, X., Peng, Q., Zhang, W., Ye, W. and Wang, H. 2020. Preparation of g-C_3N_4 nanosheets photoelectrode and its photoelectrocatalytic activity for tetracycline degradation. J. Mater. Eng., 48(12):82-89. (in Chinese)

Islam, A., Ahmad, H., Zaidi, N. and Kumar, S. 2014. Graphene oxide sheets immobilized polystyrene for column preconcentration and sensitive determination of lead by flame atomic absorption spectrometry. ACS Appl. Mater. Interfaces, 6(15): 13257-13265.

Li, H., Li, Y., Lee, M. K., Liu, Z. and Miao, C. 2015. Spatiotemporal analysis of heavy metal water pollution in transitional China. Sustainability, 7(7): 9067-9087.

Li, Z., Ma, Z., van der Kuijp, T. J., Yuan, Z. and Huang, L. 2014. A review of soil heavy metal pollution from mines in China: pollution and health risk assessment. Sci. Total Environ. 468: 843-853.

Liao, Q., Yan, S., Linghu, W., Zhu, Y., Shen, R., Ye, F., Feng, G., Dong, L., Asiri, A.M., Marwani, H.M., Xu, D., Wu, X. and Li, X. 2018. Impact of key geochemical parameters on the highly efficient sequestration of Pb (II) and Cd (II) in water using g- C_3N_4 nanosheets. J. Mol. Liq., 258: 40-47.

Shen, C., Chen, C., Wen, T., Zhao, Z., Wang, X. and Xu, A. 2015. The superior adsorption capacity of g- C_3N_4 for heavy metal ions from aqueous solutions. J. Colloid Interface Sci., 456: 7-14

Talip, Z., Eral,.M. and Hiçsönmez, Ü. 2009. Adsorption of thorium from aqueous solutions by perlite. J. Environ. Radioactiv., 100(2): 139-143.

Tian, X., Li, T., Yang, K., Xu, Y., Lu, H. and Lin, D. 2012. Effect of humic acids on physicochemical property and Cd (II) sorption of multiwalled carbon nanotubes. Chemosphere, 89(11): 1316-1322.

Wang, X., Liang, Y., An, W., Hu, J., Zhu, Y. and Cui, W. 2017. Removal of chromium (VI) by a self-regenerating and metal-free g- C_3N_4/graphene hydrogel system via the synergy of adsorption and photo-catalysis under visible light. Appl. Catal. B: Environ, 219: 53-62.

Wu, H., Chen, J., Xu, L., Guo, X., Fang, P., Du, K., Shen, C. and Sheng, G. 2021. Decorating nanoscale FeS onto metal-organic framework for the decontamination performance and mechanism of Cr (VI) and Se (IV). Colloids Surf. A: Phys. Eng. Aspects, 625: 126887.

Xu, J., Wang, H. and Liu, Y. 2016. Ecological risk assessment of heavy metals in soils surrounding oil waste disposal areas. Environ. Monit. Assess., 188(2): 125.

Zheng, W., Li, X.M., Yang, Q., Zeng, G.M., Shen, X., Zhang, Y. and Liu, J. 2007. Adsorption of Cd(II) and Cu(II) from aqueous solution by carbonate hydroxylapatite derived from eggshell waste. J. Hazard. Mater., 147(1-2): 534–539

Zhao, G., Li, J., Ren, X., Chen, C. and Wang, X.2011. Few-layered graphene oxide nanosheets as superior sorbents for heavy metal ion pollution management. Environ. Sci. Technol., 45(24): 10454-10462.

Zheng, Y., Jiao, Y., Chen, J., Liu, J., Liang, J., Du, A., Zhang, W., Zhu, Z., Smith, S.C., Jaroniec, M., Lu, G.Q. and Qiao, S. Z. 2011. Nanoporous graphitic- C_3N_4 @ carbon metal-free electrocatalysts for highly efficient oxygen reduction. J. Am. Chem. Soc., 133(50): 20116-20119.

Zhang, X., Xie, X., Wang, H., Zhang, J., Pan B. and Xie Y. 2013. Enhanced photoresponsive ultrathin graphitic-phase C_3N_4 nanosheets for bioimaging. J. Am. Chem. Soc., 135(1): 18-21.